2

Sensor Fabrication facilities, Characterization Tools and techniques

2.1 Introduction

In this chapter, we will discuss about the semiconductor device fabrication facility and related types of equipments which were used to deposit thin film materials and synthesize of nano-materials. Afterwards, different material and thin film characterization techniques like XRD, FESEM, and AFM etc. are explained to characterize the structural and morphological properties of prepared materials and thin films used to carry out the current research work. Further, we have discussed the electrical characterization facility (current versus voltage) for measuring the temperature coefficient of resistance (TCR) of Au microheater and the gas sensing performance of fabricated sensors.

2.2 Sensor fabrication facilities and related instruments

For the fabrication of our metal oxide based formaldehyde sensors and synthesis of metal oxide nanoparticles various equipment and infrastructure were used which includes clean room facilities, metallization and thin film deposition facilities, packaging machine etc. The cleanroom is an environment where temperature, humidity and airborne particles are precisely controlled. To carry out my thesis work, the clean room and infrastructure facility of the Council of Scientific and Industrial Research (CSIR) - Central Electronics Engineering Research Institute (CEERI), Pilani, Rajasthan, India, have been used. This National Research Laboratory was established on 21st September 1953 to give impetus to the research and development of electronics in the country of India. The details of the system used in this work are described in the following sections:

2.2.1 Chemical bench

For the cleaning of substrate and material, various organic chemicals (Methanol, ethanol, acetone etc.) and inorganic chemicals (sulphuric acid, chromic acid, etc.) are required. So, for these activities, we have used chemical benches, as shown in figure 2.1 (a) and (b). By using these facility, the alumina substrates were cleaned using a standard piranha cleaning method.



Figure 2.1: Chemical benches in the clean room of CSIR-CEERI, Pilani, Rajasthan, India.

2.2.2 RF Sputtering

The Radio frequency (R.F.) sputtering technique is the most commonly used physical vapor deposition technique for metal, non-metal, oxides and insulating materials. Sputtering techniques have several advantages over other physical vapour deposition (PVD) techniques, such as large area growth, thickness uniformity, low-temperature growth and low operating cost etc. Unlike other PVD techniques, the sputtering process is also carried out in a high vacuum environment. A sputtering system mainly comprises a process chamber connected with a high vacuum system, RF power supply, matching network, process gas valve and sample heaters. A 13.56 MHz RF power supply is used in RF sputtering system to couple the plasma to the target of the insulating material. For continuous plasma generation, the system frequency should be more than the effective R-C time constant. For the tuning of frequency and R-C time constant, the impedance matching network is used. The RF power is supplied to the target material through a matching network. A cleaned substrate was loaded into the process chamber with the help of load lock assembly and after loading the vacuum system started to reduce the possibility of contamination during the process. To achieve high vacuum, a vacuum system is generally equipped with a set rotary-backed turbo molecular pump. First, the rotary pump creates a rough vacuum of the order of 10^{-2} mbar and then it works as a backing source for the turbo molecular pump to attain a high vacuum of the order of 10^{-7} mbar. After achieving a high vacuum, a controlled process gas flow is inserted into the process chamber using an MFC. A substrate heater and rotation assembly are used to obtain uniform deposition over the sample.

As the vacuum level of the process chamber reaches a high value, a certain amount of inert gas or the mixture of inert and reactive gases is allowed to flow in the system and desirable working pressure is maintained with the help of a gate valve at the turbo side. The application of RF power between the target (cathode) and substrate (anode) ionized the gases present in the chamber and creates the discharge called plasma. Due to the applied field, the ions get accelerated towards the cathode and strike the target material. The continuous bombardment of ions on the target transfers the energy to the target surface and ejects the surface atoms. The dislodged atoms get deposited on the substrate placed on the anodic side. The inert gases help to get the thin film as that of the target material while mixing it with reactive gases led to thin film formation due to the reaction of reactive gas and sputtered atoms. On the other hand, the electrons emitted during bombardment help the plasma to sustain itself.

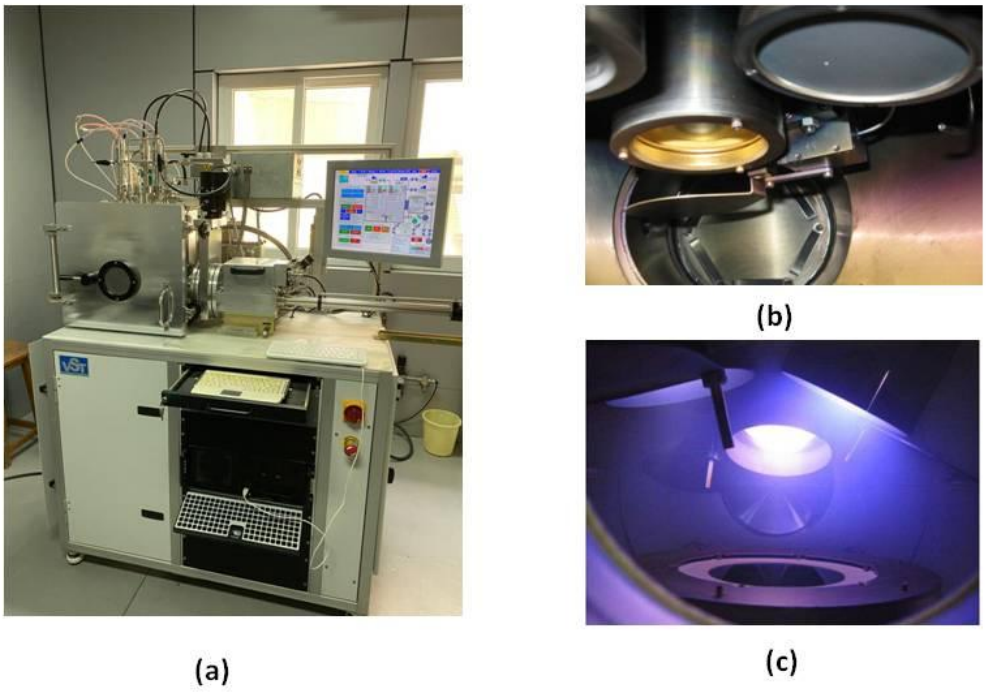

Figure 2.2: RF Sputtering system installed in the clean room of CSIR-CEERI, Pilani, Rajasthan, India. (a) Sputtering system, (b) Target fitted at the chamber of the system and (c) Ar plasma during sputtering.

Figure 2.2 (a) depicts the optical image of the RF sputtering system (TFSP-840, VST Israel) available in the clean room semiconductor fabrication facilities at CSIR-CEERI, Pilani, Rajasthan, India. The system was used to deposit gold (Au), titanium (Ti) and tin oxide (SnO_2) on the substrate (alumina and silicon wafers) during the fabrication of gas sensors in this thesis. Several depositions were carried out by varying the deposition parameters like Ar flow, RF power and time to optimize the desired film thickness to achieve the desired device performance. The optical, structural, morphological and electrical properties can be altered by deposition parameters.

2.2.3 Pulse Laser Ablation (PLA) system

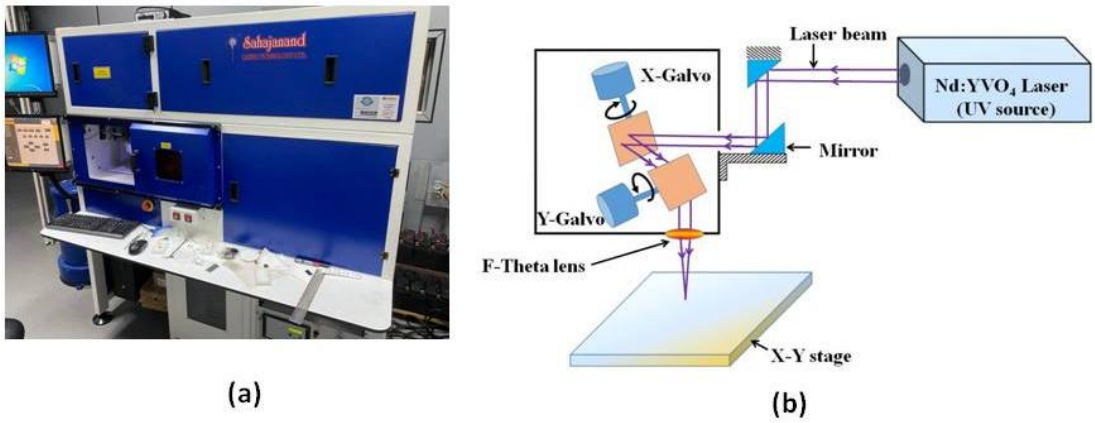

Figure 2.3: (a) Pulse Laser Ablation (PLA) system installed in the clean room of CSIR-CEERI, Pilani, Rajasthan, India and (b) Schematic diagram of the Pulse Laser Ablation (PLA) system.

A q-switched, diode-pumped solid-state ($Nd:YVO_4$) UV laser from Photonics Industries International Inc, USA was used to scribe the alumina substrate and pattern the metallization layer and also was used to synthesize the nanoparticles. During the micromachining and

micropatterning process, the operating wavelength is 355 nm at 30 KHz pulse repetition rate, 20 ns pulse width and 0.33 mJ pulse energy. A 355 nm UV laser source was selected for its high absorptivity (~ 10^6 cm^{-1}) in alumina substrate and thin film of metal. The laser power may vary from 1 mW to 10 W by adjusting the Laser Diode Driver (LDD) current. The laser beam was focused on the sample after passing through the beam expander, beam bender, galvomirrors and f-theta-lens (focal length of 90 mm) to get a spot size of 20 µm. A two-axis (U, V) high-speed galvomirrors was used to change the laser beam position during patterning of metal layer. The sample was mounted on a highly precision X-Y translating stage controlled by a CNC controller through g-code programming which was written in a personal computer. The focusing system of the lenses is adjusted by a liner z movement. The laser beam was focused by varying the Z-axis movement in which galvomirrors and f-theta-lens were attached. The focusing point was determined by a CCD (charge-coupled devices) camera which is attached to the Z -position control system as shown in figure 2.3 (a). The schematic diagram is shown in figure 2.3 (b).

2.2.4 Annealing furnace & Oven

The annealing furnace has been used to anneal the sensing material for a long time. Figure 2.4 shows the annealing furnace which has heen used during my research work.

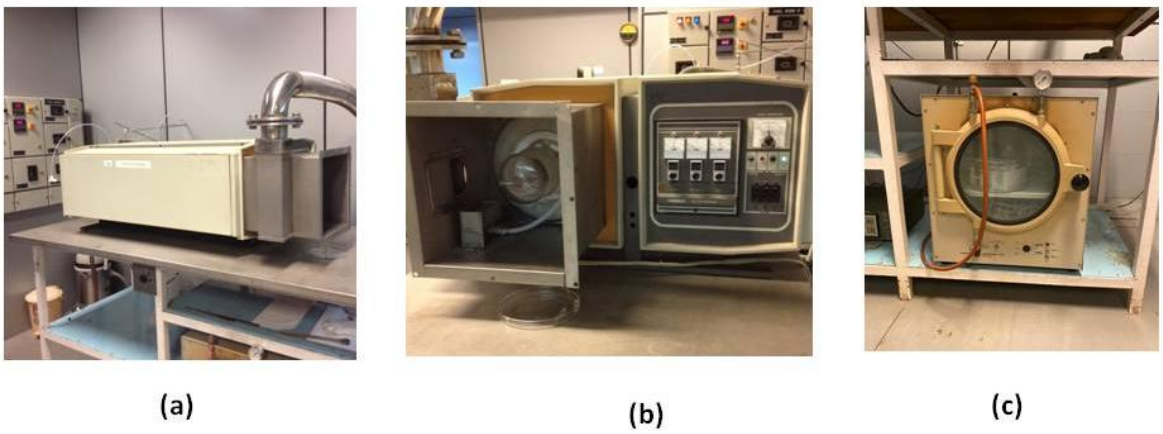

Figure 2.4: Annealing furnace (a) side view and (b) front view. (c) Oven.

2.2.5 Wire bonding machine

This machine has been used during the packaging and bonding of sensors. The photographic image of the wire bonding machine (Hybond) is depicted in figure 2.5 (a).

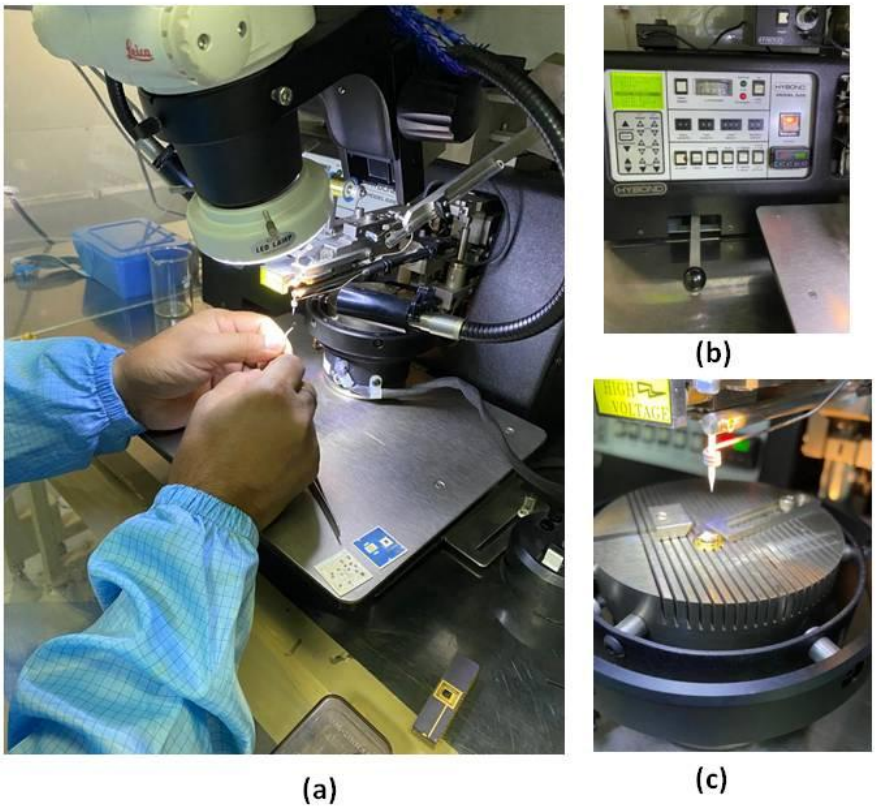

Figure 2.5: Wire bonding machine (Hybond) at CSIR-CEERI, Pilani, Rajasthan, India: (a) machine (b) control panel, and (c) bonding tool.

2.3 Material Characterization Tools and Techniques

In this work, various types of characterization techniques were involved for material and thin film characterization to analyze the structural, morphological, optical and electrical properties. The basic principle and brief description of the instruments used are given in the following sections.

2.3.1 Surface Profiler and Sheet Resistance Measurement System

The surface profiler is the commonly used instrument to create the 2-D and 3-D images of the surface profile. The surface profiling is done by using a sharp stylus moving along the surface of the sample to measure the different properties like height, roughness, stress and strain. A feedback loop communicates the change in the force exerted on the stylus during the scan; The feedback loop helps to maintain constant stylus force during the scan. The surface profiler works in contact mode for the input parameters like stylus force, scan time and scan area. The contact mode measurement can create surface damage on highly sensitive soft materials. In this work, the surface profiler (DektakXt, Bruker) is used to measure the thickness of deposited thin films by scanning them for height profile. During the work, the stylus used had a diameter of 2 μm and the samples were scanned in hills and valley configurations. The pictorial image is depicted in figure 2.6 (a).

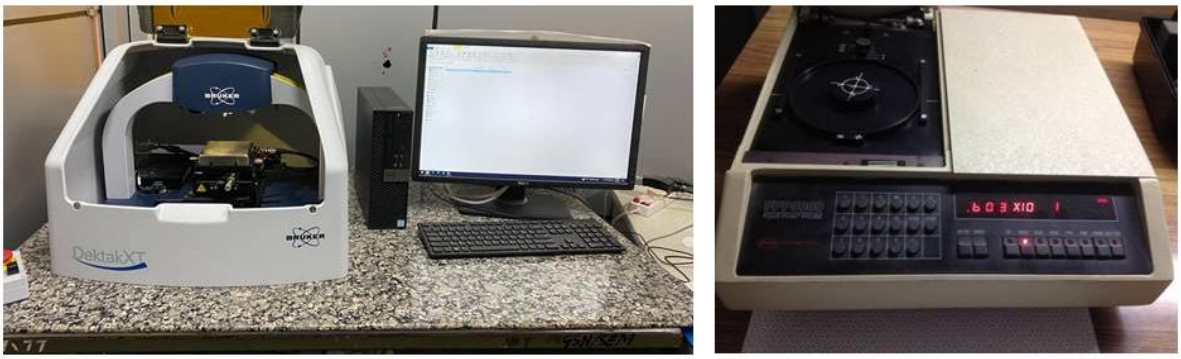

(a) (b)

Figure 2.6: (a) Surface profiler for thickness measuring system (DektakXt, Bruker) and (b) Sheet-resistance measurement system (VEECO FPP-5000).

The sheet resistance of the metal thin films was determined by the 4-point probe (VEECO FPP-5000) machine. Figure 2.6 (b) shows the optical image of sheet resistance measurement system.

2.3.2 X-ray Diffraction (XRD) system

XRD is a core and the most explored technique for structural properties analysis of the material and thin film. It provides information on different structural properties like lattice parameters, orientation, phase, composition and grain size for a subjected material or thin film. The XRD system mainly comprises of X-ray generator, collimator and detector. The X-ray generator generates the X-rays using a cathode ray tube, which contains the source material like copper. The generated X-ray passes through the filter assembly to get the monochromatic characteristic X-ray (Kα), for the copper source. The wavelength of the characteristics X-ray is 1.54 Å. The X-ray is directed towards the sample passing through the collimator to scan the sample for 2θ angles. The X-ray diffracted from the sample detected at the detector side and processed to generate the XRD pattern. The principle of XRD is based on constructive interference of X-rays from the crystalline planes of the specimen. Bragg's equation is the primary and must condition for constructive interference given as:

$$n\lambda = 2dsin\theta \qquad (2.1)$$

Where λ is the wavelength of characteristic X-ray, d is the lattice spacing for the sample, n is the order of diffraction and θ is the diffraction angle. Condition of constructive interference is n=1. Figure 2.7 (c) is a representation of the law of diffraction. From figure 2.7 (c), we can understand Bragg's law and can find the value of lattice spacing d using the known value of other parameters mentioned in the equation [2.1].

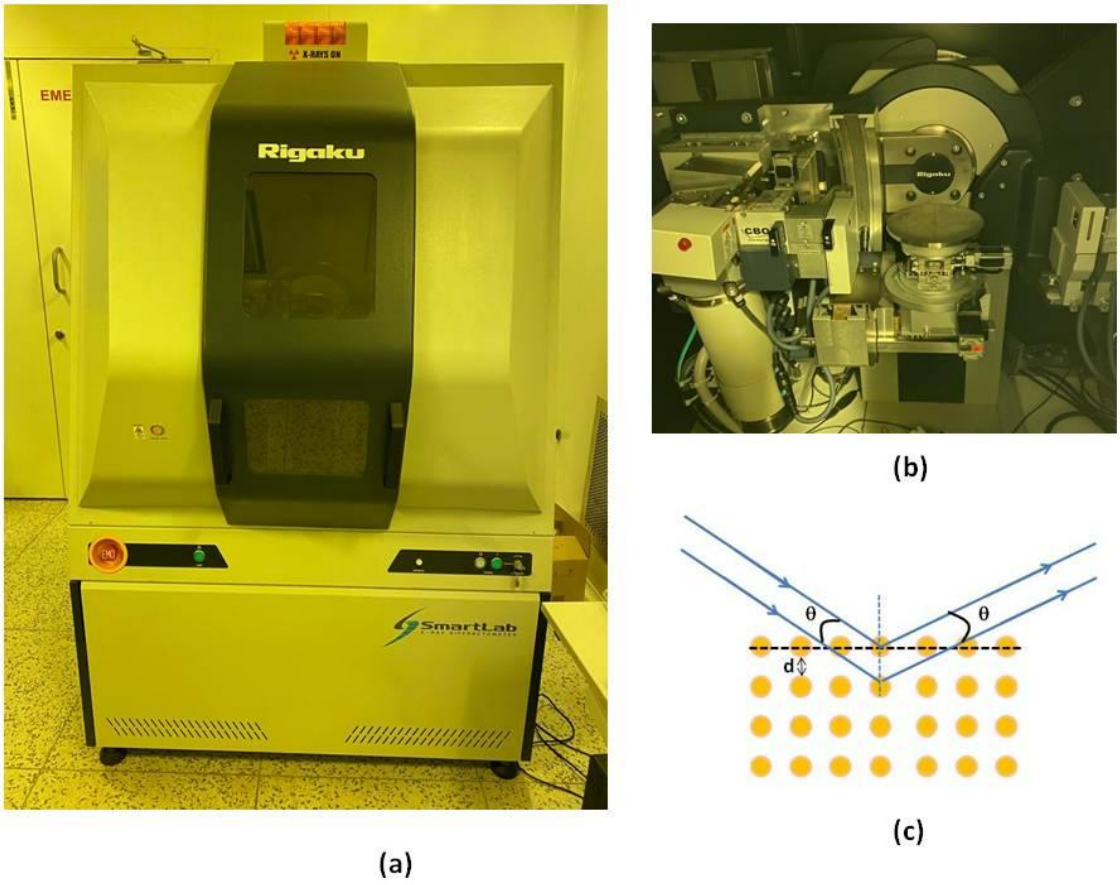

Figure 2.7: XRD system (Rigaku SmartLab, Rigaku Corporation, Tokyo, Japan) in the clean room of CSIR-CEERI, Pilani, Rajasthan, India : (a) XRD System (b) Stage and (c) Schematic diagram of XRD mechanism.

In this thesis work, the XRD system (Rigaku SmartLab, Rigaku Corporation, Tokyo, Japan) as depicted in figure 2.7 (a) was used to obtain the structural properties of synthesized nanoparticles. The system is a part of the device characterization facility at CSIR-CEERI, Pilani, Rajasthan, India. The system uses a copper source to generate an X-ray of wavelength Cu Kα =1.54 Å.

2.3.3 Atomic Force Microscopy (AFM)

AFM is a commonly explored microscopic technique to observe the nanoscale surface morphology of thin films. The force that appeared between the probe and the surface of the sample plays a role in detecting the different morphological characteristics. In the AFM system, a sharp AFM tip of diameter 10-20 nm attached to a cantilever connected with a piezo element scans the sample surface in a raster scan pattern. The oscillation and Z-plane movement of the cantilever over the surface is enabled by the piezo element and the piezo motor controls the XY movement of the sample. The force exerted between the tip and sample creates the deflection in the cantilever. The deflection in the reflected laser positioned at the back side of the cantilever due to deflection in the cantilever is observed as a change in the photocurrent of the photodiode. AFM works in three different modes: contact mode, tapping mode and noncontact mode. In contact mode, the tip moves in contact with the surface and the force induced deflects the cantilever. For contact mode AFM, a cantilever with low stiffness is used to avoid surface damage. In tapping mode, the tip scans the surface with a resonant frequency and makes contact with the surface only at the bottom of the amplitude. Tapping mode creates lesser damage than the contact mode as the amplitude and time of applied force are very less in comparison to contact mode. In non-contact mode, the tip is set at a particular height over the

surface and scans the surface. When the tip reaches the proximity to the surface, various forces associated between the tip and surface come into the picture. The variation in the height profile due to the inducing force between the tip and surface due to the surface profile causes the deflection in the cantilever. The distance between the AFM tip and the sample surface is defined as the set point in a typical AFM system. To maintain the constant distance between the tip and the surface a feedback loop is used. A photodetector in the system can measure the smallest deflection as low as 0.1 Å. The oscillation in the cantilever due to the surface profile while keeping the force constant gives the topographic image.

In this work, AFM (Innova, Bruker) was used to obtain the surface topography of deposited thin films. All the scans were performed in the non-contact mode for a scan rate of 0.75 Hz. The topographic images were further analyzed to obtain different morphological information. Figure 2.8 depicts the pictorial image of the AFM image used during the work.



Figure 2.8: Atomic Force Microscopy (AFM) in the clean room of CSIR-CEERI, Pilani, Rajasthan, India.

2.3.4 Field Emission Scanning Electron Microscopy (FESEM)

FESEM is a powerful and popular technique to analyze the surface morphology, size of particles or nanostructures, nanostructured shapes and the thickness of the nanometric thin films. The working principle of FESEM and SEM is almost the same except for the difference in electron emission technique. The SEM use a thermionic emission gun to produce electron, while FESEM uses a field emission electron gun which offers a focused electron beam of a wide energy range to provide a detailed and high-resolution image of surface features. The imaging at a low potential is an added advantage of FESEM over SEM, which enables it to image non-conducting samples by reducing the charging effect. The incident electrons interact with the surface of the sample and emit the backscattered and secondary electrons. These emitted electrons are detected by detectors and create the surface image. The backscattered electrons provide the details of the surface defects or dissimilarities in a sample while secondary electrons help to generate the topographic and morphological behavior of the samples.

In a FESEM system, the field emission gun generates the electron in an ultra-high vacuum and the field gradient helps to accelerate these electrons to pass through various electromagnetic lenses to focus them on the sample surface. The interaction of electrons on the surface of the sample emits the backscattered and secondary electrons. The emitted electrons are detected at their respective detectors and processed to get the sample information in the form of a high-resolution image. In this work, the FESEM (FEI, Apreo) was used to obtain the morphological details of the deposited thin films. Figure 2.9 depicts the pictorial image of the FESEM used to carry out the presented work.

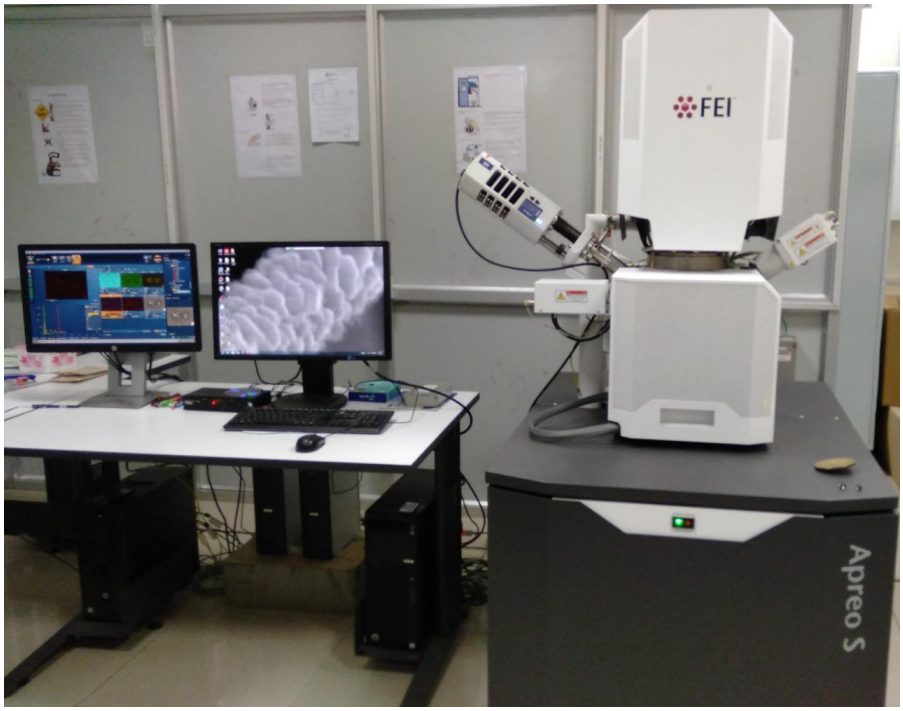

Figure 2.9 : FESEM characterization facility (FEI, Apreo) in the clean room of CSIR-CEERI, Pilani, Rajasthan, India.

2.3.5 Thermal Imaging Camera

Measurement of the heat distribution profile and heat gradient of the fabricated sensor platform is very important during the characterization of microheater platform. For this purpose, infrared based thermal imaging camera with high resolution has been commonly used.



Figure 2.10 : Thermal imaging camera (AT-Automation Technology GmbH infra red based camera) installed at CSIR-CEERI, Pilani, Rajasthan, India : (a) side view and (b) close view.

In this work, AT-Automation Technology GmbH infra red based camera was used to measure the heat distribution profile of the microhotplate platform during the optimization of sensing temperature of metal oxide based sensors. Figure 2.10 (a) and (b) represent the photograph of the thermal imaging camera used during work.

2.4 TCR measurement System

The temperature coefficient of resistance (TCR) of the Au microheater was analyzed by a Semiconductor Characterization System (Keithley 4200 SCS). The system has the capability to perform two probes, three probes and four probes I-V measurements. The system is equipped with a temperature controlled chuck in which temperature of the chuck can be varied from room temperature to 200°C. TCR value of the Au microheater can also be measured with this system. A simple graphical user interface helps to control the input parameter to perform the measurement. The SCS is connected to a probe station (PM5 Suss Microtech) to take connections from devices. The probe station tips are connected to SCS via coaxial cables to send input signals and measure output signals. The figure 2.11 (a) depicts the Keithley 4200 SCS and figure 2.11 (b) shows the temperature controller unit attached to the system chuck.

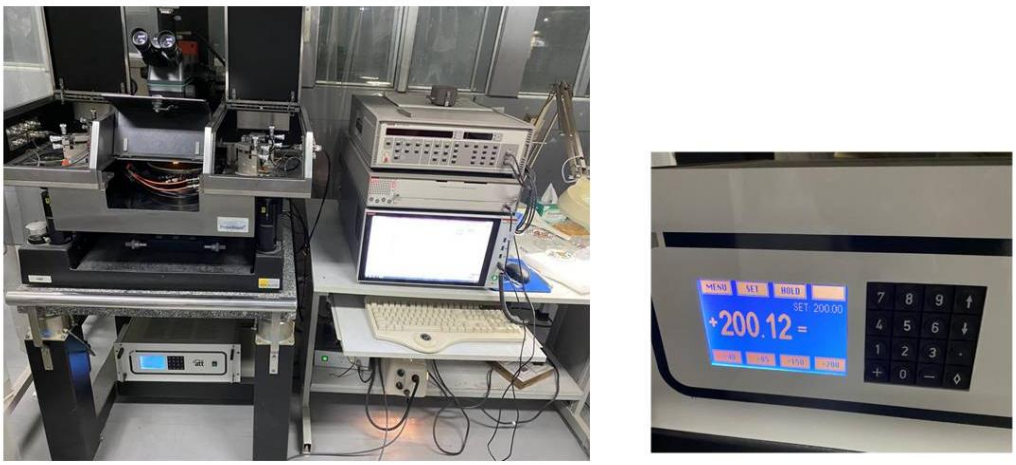

(a) (b)

Figure 2.11: Probe station with Keithley-4200 SCS for electrical characterization at CSIR-CEERI, Pilani, Rajasthan, India.

2.5 Computer controlled LabVIEW based gas sensor test set-up

The schematic of gas sensing test set-up is shown in figure 2.12 which is used for this thesis work. After the fabrication of the gas sensors, they were put into the gas sensing test chamber to study the gas sensing performance. There are two ways to investigate the gas sensing characteristics of any device: (1) Dynamic gas sensing, and (2) Static gas sensing. In dynamic gas sensing, sensor is exposed continuously with a particular concentration of gas and goes out from another side of the gas chamber continuously. On the other hand, in static gas sensing, a device is put in a closed gas chamber and the desired gas concentration is injected into the chamber and gas is carried out from the chamber after saturating the effect of gas on the device. In this thesis work, we followed static gas sensing procedure and the gas sensing properties of the sensor was performed by placing the sensor in an air-proof glass chamber (~ 2.3 L in volume). The glass chamber has a top glass lid with a hole to insert the liquid analyte VOCs sources into the chamber. The glass chamber was placed on a hotplate and the temperature of the hotplate was set to 70°C. The schematic diagram of the gas sensor test setup is shown in figure 2.12 (b). During the testing, the temperature was provided by the integrated

microheater as the metal oxide sensor works at elevated temperature and for that purpose, a source measure unit (Agilent E3632A) was connected across the microheater to pass the constant current. To obtain a stable base line resistance during the gas sensing performance test, the sensor needs to heat continuously for a long duration (more than two days). During the gas sensing performance test, the ambient air was used as a reference and diluting gas for both cases. A digital multimeter (Keithley 2001) interfaced with a personal computer (PC) was used to measure the change in resistance during the gas sensing performance test and during testing, real-time data was recorded in a personal computer via a custom-built LabVIEW program (Figure 2.12 (b)).

To obtain the desired concentration of Volatile Organic Compounds (VOCs) such as methanol, ethanol, acetone, isopropanol and trichloroethylene (TCE) etc, a pre-determined amount of electronic grade (≥ 99.8% pure) liquid analytes sources were injected into the glass chamber via the hole of top glass lid using a micropipette [Gaca et al., 2014][Li et al., 2017b]. But, in the thesis work during the gas sensing performance test, a commercially available formalin solution (37 wt.% in H_2O) was used as a source of formaldehyde gas. The 37 wt.% formalin solution was diluted by adding more water to prepare the diluted solution, and this diluted solution was injected inside the test chamber as a liquid analyte. After the injection of the liquid analyte, it came into contact with the hot glass wall of the chamber and rapidly, the liquid was vaporized. In the test chamber, the desired concentration of volatile organic compounds (VOCs) was obtained via the following formula (2.2) [Wang et al., 2014][Wang et al., 2012]:

$$C = \frac{22.4\rho T V_S}{273MV} \times 10^3 \qquad (2.2)$$

where C is formaldehyde concentration in ppm, ρ is the density of the liquid formalin in g/ml, T is the temperature of the glass chamber in Kelvin, V_S is the volume of liquid formalin solution in µL, M is the molecular weight of formalin solution in g/mol, and V is chamber volume in litre.

In our thesis work, the sensor response (β) towards analyte gas was defined as the ratio ($\beta = R_a / R_g$) of sensor resistance in the air (R_a) to the sensor resistance in the analyte gas environment (R_g). During the gas sensing performance test, the response time (τ_{res}) and recovery time (τ_{rec}) was determined as the time taken by the sensor to change the resistance value of the sensor from its initial value (10%) to 90% of the final change in resistance during adsorption and desorption of test gases [Wu et al., 2012][Li et al., 2019a].

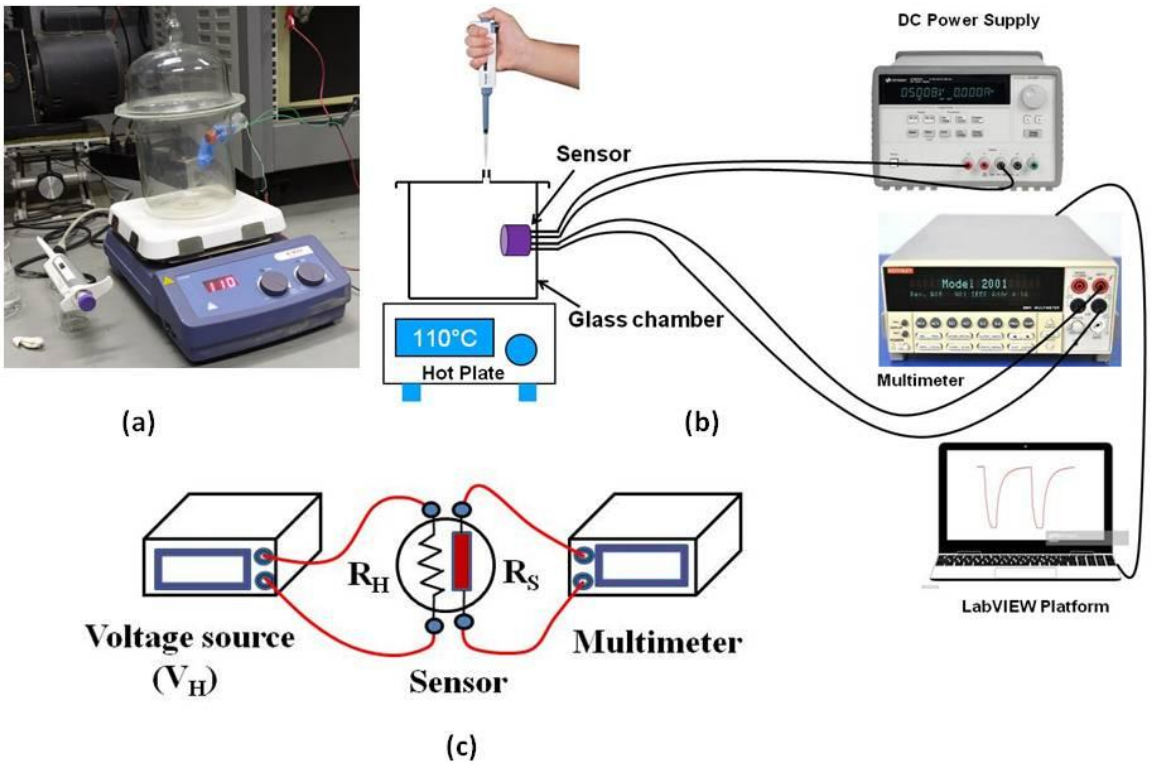

Figure 2.12: Computer controlled LabVIEW based gas sensor test set-up at CSIR-CEERI, Pilani, Rajasthan, India. (a) Glass made test chamber, (b) Schematic of connection diagram interfaced with instruments and LabVIEW based measurement system and (c) Schematic of the circuit diagram with instruments connected with sensor and microheater.

…